

**Liangbiao Wang^{1,*}, Dejian Zhao¹, Qinglin Cheng¹,
Quanquan Lu¹, Weiqiao Liu¹, Keyan Bao², Binglong Zhu¹,
Quanfa Zhou^{1,**}**

¹Jiangsu Key Laboratory of Precious Metals Chemistry
and Engineering, School of Chemistry and Environment Engineering,
Jiangsu University of Technology, Changzhou 213001, P. R. China

²College of Chemistry and Pharmacy Engineering,
Nanyang Normal University, Nanyang, Henan 473061, P. R. China

*lbwang@jsut.edu.cn

**labzqf@jsut.edu.cn

Iodine-assisted solid-state synthesis and characterization of nanocrystalline zirconium diboride nanosheets

A solid-state route was developed to prepare zirconium diboride nanosheets with the dimension of about 500 nm and thickness of about 20 nm from zirconium dioxide, iodine and sodium borohydride at 700 °C in an autoclave reactor. The obtained ZrB₂ product was investigated by X-ray diffraction, scanning electron microscope and transmission electron microscopy. The obtained product was also studied by thermogravimetric analysis. It had good thermal stability and oxidation resistance below 400 °C in air. Furthermore, the possible formation mechanism of ZrB₂ was also discussed.

Keywords: solid-state route, X-ray diffraction, zirconium diboride, nanosheets, chemical synthesis.

INTRODUCTION

Transition metal borides had attracted consideration interests because of their excellent properties, such as high melting point, high chemical stability, good electrical and thermal conductivity, and high hardness [1–4]. These various unique properties presented a wide range of applications, such as refractory lining materials, cutting tools, electronic materials and aerospace technologies. Among these, zirconium diboride (ZrB₂) was used widely in high temperature environments due to its high melting point (3245 °C), high thermal conductivity (57.9 W·m⁻¹·K⁻¹), high hardness (22 GPa), low density (6.10 g/cm³), and good corrosion resistance [5, 6]. In addition, ZrB₂ was a superconductor with a very sharp superconducting transition at 5.5 K [7].

Up to now, several synthetic methods had been developed to synthesize ZrB₂ materials, such as, the carbothermal reduction of zirconium dioxide and boron carbide (B₄C) at 1400 °C [8], self-propagating high temperature synthesis (SHS) [9], high temperature reaction from a ZrO₂–C–BN precursor [10], solid-state reduction of zirconium dioxide and boron oxide by a metallic reducing agent (such as magnesium or aluminum) at temperatures of about 1500 °C [11] and the mechanochemistry treatment of zirconia and amorphous boron at 1100 °C [12]. ZrB₂ can

also be prepared by chemical vapor deposition (CVD) from $ZrCl_4$, H_2 and BCl_3 [13]. Amorphous $ZrB_{2.76}$ was also obtained by thermolysis of zirconium precursor ($Zr(BH_4)_4$) [14]. A general route towards metal boride nanocrystals had been developed by ionothermal process at a relatively mild temperature (500–900 °C) [15]. ZrB_2 can also be obtained by a co-reduction method at low temperature [16, 17]. Very recently, a solid-state reaction between zirconium dioxide and sodium borohydride was reported to produce pure nanosized ZrB_2 at the temperature of 1100 °C [18]. Herein, we reported a solid-state reaction of zirconium dioxide and solid borohydride with iodine assisted to produce ZrB_2 nanosheets at the temperature of 700 °C in an autoclave.

EXPERIMENTAL

All the reagents used in the experiments were purchased from Shanghai Chemical Reagents Company. All manipulations in our experiments were carried out in a glove box purged with flowing argon gas. In a typical procedure, zirconium dioxide (0.25 g), iodine (0.54 g) and sodium borohydride (0.76 g) were put into a stainless steel autoclave of 20 mL capacity. The autoclave was sealed and heated in an electric stove with a heating ramp rate of 10 °C/min from room temperature to 700 °C. The autoclave was maintained at 700 °C for 10 h, and then followed by cooling to room temperature in the furnace naturally. The product collected from the autoclave was washed by absolute ethyl alcohol, distilled water and dilute HCl aqueous solution for several times to remove the impurities. Finally the final product was dried under vacuum at 60 °C for 10 h for further characterization.

X-ray diffraction (XRD) pattern of the obtained product was performed with a Philips X'Pert X-ray powder diffractometer using $CuK\alpha$ radiation ($\lambda = 1.54178 \text{ \AA}$). The microstructure of the obtained product was investigated with a field-emitting scanning electron microscope (FE-SEM, JEOL-JSM-6700F), a transmission electron microscope (TEM, H7650), and a high-resolution transmission electron microscope (HRTEM, JEOL-2010) with an accelerating voltage of 200 kV. Thermogravimetric analysis (TGA) profile was performed on a Shimadzu-50 thermoanalyzer apparatus under flowing air and argon below 1000 °C at a rate of 10 °C/min.

RESULTS AND DISCUSSION

XRD was used to check the crystal structure and the phase purity of the obtained product. A typical XRD pattern of the obtained product was shown in Fig. 1. All the peaks in Fig. 1 of the (001), (100), (101), (002), (110), (102), (111), (200), and (201) reflections can be indexed to pure hexagonal ZrB_2 with lattice constants of $a = 3.169 \text{ \AA}$ and $c = 3.543 \text{ \AA}$, which were consistent with the reported values of hexagonal ZrB_2 (Joint Committee on Powder Diffraction Standards (JCPDS) cards, No. 65-3389). No impurity peaks from ZrO_2 or Zr were detected in Fig. 1, suggesting the ZrB_2 product with high purity. All the peaks with strong diffraction intensity indicated the obtained ZrB_2 with excellent crystallinity.

FE-SEM, TEM and HRTEM were used to study the microstructure of the obtained ZrB_2 product. The FE-SEM image of the obtained ZrB_2 is shown in Figs. 2, *a* and *b*. The FE-SEM image (see Fig. 2, *a*) revealed that the ZrB_2 product was composed of nanosheets and nanoparticles. A high-magnification image (see Fig. 2, *b*) showed that the obtained ZrB_2 product was composed of hexagonal plate and irregular nanosheets. The TEM image (Fig. 3, *a*) of the ZrB_2 product showed the dimension of zirconium diboride (ZrB_2) nanosheets was about 500 nm with thickness of about 20 nm on average. In the HRTEM image (see Fig. 3, *b*), the

obvious lattice fringes of hexagonal ZrB_2 indicated that the obtained ZrB_2 product was well crystalline. The plane intervals was measured to be about 0.22 nm, which corresponded to the separation between (101) lattice planes of hexagonal ZrB_2 .

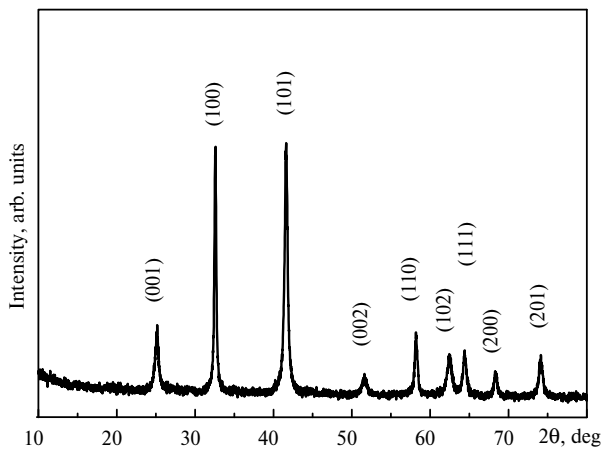


Fig. 1. XRD pattern of the obtained ZrB_2 .

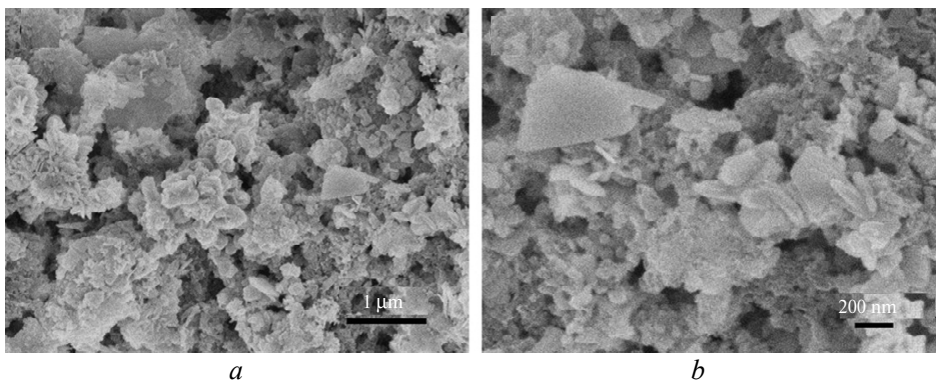


Fig. 2. FE-SEM images of the obtained ZrB_2 product: low-magnification image (a), high-magnification image (b).

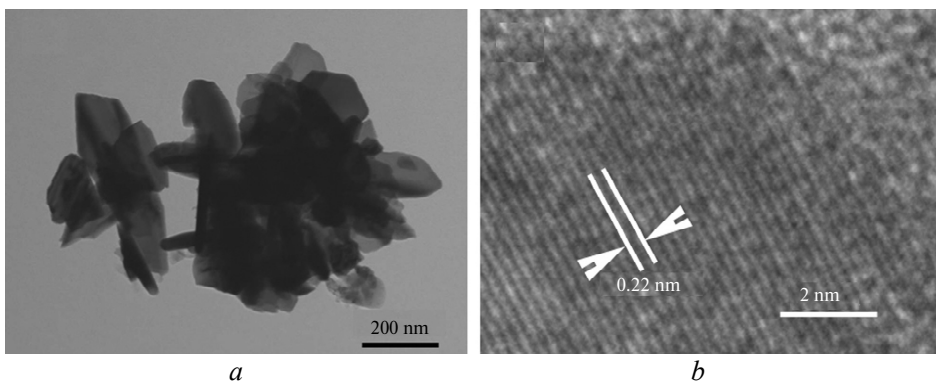


Fig. 3. TEM image of ZrB_2 nanosheets (a), HRTEM image of ZrB_2 nanosheets (b).

The thermal stabilities and oxidation resistances of materials determine their application conditions. Thus, it is very important to study the thermal stability and oxidation resistance of the obtained ZrB_2 product. The TGA of the ZrB_2 is shown

in Fig. 4. The TGA was carried out from room temperature to 1000 °C with a heating ramp rate of 10 °C/min under flowing air and argon gases. The weight of the product from room temperature to 1000 °C under the flowing air is shown in the curve 1. The TGA curve 1 shows that the weight of the product had not changed below 400 °C. When the temperature is over 400 °C, the ZrB₂ product begins to oxidize to zirconium dioxide (ZrO₂) and diboron trioxide (B₂O₃). The weight increment was about 55.2 % by converting the ZrB₂ into zirconium dioxide (ZrO₂) and diboron trioxide (B₂O₃). The weight of the ZrB₂ product from room temperature to 1000 °C under the flowing argon gas is shown in the curve 2, which shows that the weight of the product was almost unchanged below 1000 °C. The ZrB₂ product obtained by our designed route had anti-oxidation behaviour under 400 °C and good thermal stability.

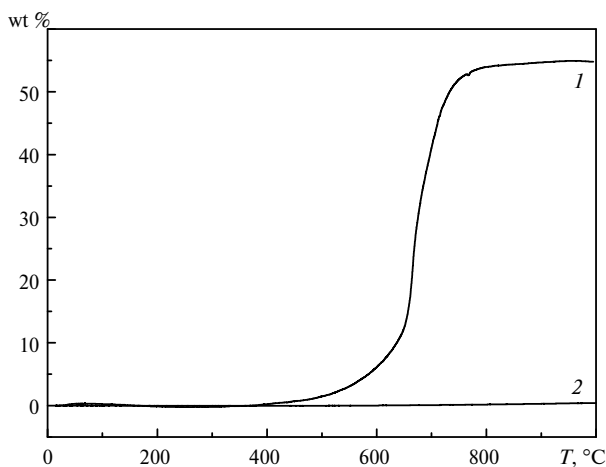


Fig. 4. TGA profile of the ZrB₂ product under flowing air (1) and argon (2).

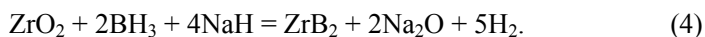
The possible formation mechanism of ZrB₂ can be proposed here. The reaction between ZrO₂ and NaBH₄ used to produce ZrB₂ was highly exothermic, but the reaction was initiated at high temperature of 1100 °C. In our experimental process, the mole ratio of the raw materials is ZrO₂:I₂:NaBH₄ = 1:1:10. With the assistance of iodine, hexagonal ZrB₂ nanosheets were prepared from ZrO₂ and NaBH₄ in an autoclave, in which the exothermic reaction between iodine and NaH (coming from the pyrolysis of NaBH₄) led to the formation of ZrB₂ nanosheets at a relatively low temperature. The solid-state synthesis of crystalline ZrB₂ by the reaction of ZrO₂ and NaBH₄ with I₂ assisted in an autoclave can be described as follows



When the temperature increased over 500 °C, the NaBH₄, as the boride source, decomposed to BH₃ and NaH, which is shown in Eqs.



The possible formation process of ZrB₂ nanosheets could be illustrated as follows



According to free energy calculations of the Eq. (3), the present solid state reaction is highly exothermic ($\Delta_r H_m = -462.84$ kJ/mol). A great deal of heat generated from the reaction of NaH and iodine and resulted in a high temperature in an autoclave, which favored crystallization of ZrB₂. Meanwhile, H₂ as byproduct coming from the Eq. (1) can bring high pressure in the autoclave, which is also beneficial to the formation of crystalline ZrB₂. The influence of iodine and reaction temperature on the formation of ZrB₂ was investigated. The optimal reaction temperature is 700 °C. Although the present synthetic route is thermodynamically spontaneous, pure ZrB₂ could not be obtained at the temperature of 600 °C. In addition, iodine played a key role in the formation of ZrB₂ nanosheets. ZrB₂ cannot be obtained by the reaction of ZrO₂ and NaBH₄ at 700 °C.

CONCLUSIONS

In summary, ZrB₂ nanosheets with the dimensions of about 500 nm and thickness of about 20 nm were successfully prepared at 700 °C in an autoclave by using zirconium dioxide, sodium borohydride and iodine as reactants. The ZrB₂ nanosheets obtained by the designed route have anti-oxidation behaviour under 400 °C and good thermal stability. In comparison with previous synthetic routes, the present route has the advantages of utilizing inexpensive starting materials, simple apparatus and simple operation.

ACKNOWLEDGEMENTS

This work was supported by Natural Science Foundation of Jiangsu Province (No. BK20160292), Natural Science Foundation of the Higher Educations Institutions of Jiangsu Province (No. 16KJB150013), the National Natural Science Foundation of China (No. U1404505), the Program for Innovative Talent in University of Henan Province (16HASTIT010).

Розроблено твердотільний напрямок отримання наношарів дибориду цирконію розміром ~ 500 нм і товщиною ~ 20 нм з діоксиду цирконію, йоду та боргідриду натрію при 700 °C в автоклавному реакторі. Отриманий продукт ZrB₂ досліджували рентгенівською дифракцією, скануючим електронним мікроскопом і трансмісійною електронною мікроскопією. Отриманий продукт також вивчали термогравіметричним аналізом. Він мав гарну термостійкість і стійкість до окиснення нижче 400 °C на повітрі. Крім того, обговорено також можливий механізм утворення ZrB₂.

Ключові слова: твердотільна схема, рентгенівська дифракція, диборид цирконію, нанорозміри, хімічний синтез.

Разработан твердотельный путь получения нанослоев диборида циркония размером ~ 500 нм и толщиной ~ 20 нм из диоксида циркония, йода и боргидрида натрия при 700 °C в автоклавной реакторе. Полученный продукт ZrB₂ исследовали рентгеновской дифракцией, сканирующим электронным микроскопом и трансмиссионной электронной микроскопией. Полученный продукт также изучали термогравиметрическим анализом. Он имел хорошую термостойкость и устойчивость к окислению ниже 400 °C на воздухе. Кроме того, обсуждали также возможный механизм образования ZrB₂.

Ключевые слова: твердотельная схема, рентгеновская дифракция, диборид циркония, наноразмеры, химический синтез.

1. Adams R. M. Boron, metallo-boron compounds and boranes. – New York: Interscience, 1964.
2. Samsonov G. V., Vinitiskii I. M. Handbook of refractory compounds. – New York: Plenum Press, 1980.
3. Zhang G. J., Ji Z., Ni D. W., Liu H. T., Kan Y. M. Boride ceramics: densification, microstructure tailoring and properties improvement // J. Inorg. Mater. – 2012. – 27, N 3. – P. 225–233.

4. *Upadhya K., Yang J. M., Hoffman W. P.* Materials for ultrahigh temperature structural applications // *Am. Ceram. Soc. Bull.* – 1997. – **76**, N 12. – P. 51–56.
5. *Fahrenholtz W. G., Hilmas G. E.* Refractory diborides of zirconium and hafnium // *J. Am. Ceram. Soc.* – 2007. – **90**, N 5. – P. 1347–1364.
6. *Ni D. W., Zhang G. J., Kan Y. M., Sakka Y.* Highly textured ZrB₂-based ultrahigh temperature ceramics via strong magnetic field alignment // *Scripta Mater.* – 2009. – **60**, N 8. – P. 615–618.
7. *Gasparov V. A., Sidorov N. S., Zver'kova I. I., Kulakov M. P.* Electron transport in diborides: Observation of superconductivity in ZrB₂ // *JETP Lett.* – 2001. – **73**, N 10. – P. 532–535.
8. *Zhao H., He Y., Jin Z. Z.* Preparation of zirconium boride powder // *J. Am. Ceram. Soc.* – 1995. – **78**, N 9. – P. 2534–2536.
9. *Camurlu H. E., Maglia F.* Self-propagating high-temperature synthesis of ZrB₂ or TiB₂ reinforced Ni–Al composite powder // *J. Alloys. Comps.* – 2009. – **478**, N 1–2. – P. 721–725.
10. *Yan C. L., Liu R. J., Zhang C. R., Cao Y., Long X.* Synthesis of ZrB₂ powders from ZrO₂, BN, and C // *J. Am. Ceram. Soc.* – 2016. – **99**, N 1. – P. 16–19.
11. *Schwarzkopf P., Kieffer R.* Refractory hard metals. – New York: MacMillan Co., 1953.
12. *Setoudeh N., Welham N. J.* Formation of zirconium diboride (ZrB₂) by room temperature mechanochemical reaction between ZrO₂, B₂O₃ and Mg // *J. Alloys. Compd.* – 2006. – **420**, N 1–2. – P. 225–228.
13. *Reich S. S., Hanko K., Szepes L.* Deposition of thin-films of zirconium and hafnium boride by plasma enhanced chemical vapor-deposition // *Adv. Mater.* – 1992. – **4**, N 10. – P. 650–653.
14. *Andrievskii R. A., Kravchenko S. E., Shikin S. P.* Preparation and some properties of ultrafine zirconium boride and titanium boride powders // *Inorg. Mater.* – 1995. – **31**, N 8. – P. 965–968.
15. *Portehault D., Devi S., Beaunier P., Gervais C., Giordano C., Sanchez C., Antonietti M.* A general solution route toward metal boride nanocrystals // *Angew. Chem. Int. Edit.* – 2011. – **50**, N 14. – P. 3262–3265.
16. *Chen L. Y., Gu Y. L., Shi L., Ma J., Yang Z.* Low-temperature synthesis of nanocrystalline ZrB₂ via Co-reduction of ZrCl₄ and BBr₃ // *Bull. Chem. Soc. Jpn.* – 2004. – **77**, N 7. – P. 1423–1424.
17. *Zhu Y. C., Li Q. W., Mei T., Qian Y.* Solid state synthesis of nitride, carbide and boride nanocrystals in an autoclave // *J. Mater. Chem.* – 2011. – **21**, N 36. – P. 13756–13764.
18. *Zoli L., Costa A. L., Sciti D.* Synthesis of nanosized zirconium diboride powder via oxide-borohydride solid-state reaction // *Scripta Mater.* – 2015. – **109**. – P. 100–103.

Received 13.02.17